Computers in Biology and Medicine 107 (2019) 227–234

Contents lists available at ScienceDirect

Computers in Biology and Medicine

journal homepage: www.elsevier.com/locate/compbiomed

ColocalizR: An open-source application for cell-based high-throughput colocalization analysis

Allan Sauvat[a,b,c,d,e,1], Marion Leduc[a,b,c,d,e,1], Kevin Müller[a,b,c,d,e], Oliver Kepp[a,b,c,d,e], Guido Kroemer[a,b,c,d,e,f,g,h,*]

[a] Université Paris Descartes, Sorbonne Paris Cité, Paris, France
[b] Equipe 11 Labellisée Ligue Nationale Contre le Cancer, Centre de Recherche des Cordeliers, Paris, France
[c] Institut National de la Santé et de la Recherche Médicale, U1138, Paris, France
[d] Université Pierre et Marie Curie, Paris, France
[e] Metabolomics and Cell Biology Platforms, Gustave Roussy Cancer Campus, Villejuif, France
[f] Faculty of Medicine, University of Paris Sud, Kremlin-Bicêtre, France
[g] Pôle de Biologie, Hôpital Européen Georges Pompidou, AP-HP, Paris, France
[h] Department of Women's and Children's Health, Karolinska University Hospital, Stockholm, Sweden

ARTICLE INFO

Keywords:
Fluorescence microscopy
Co-occurrence
Co-distribution
Cellular imaging
Systems biology

ABSTRACT

The microscopic assessment of the colocalization of fluorescent signals has been widely used in cell biology. Although imaging techniques have drastically improved over the past decades, the quantification of colocalization by measures such as the Pearson correlation coefficient or Manders overlap coefficient, has not changed. Here, we report the development of an R-based application that allows to (i) automatically segment cells and subcellular compartments, (ii) measure morphology and texture features, and (iii) calculate the degree of colocalization within each cell. Colocalization can thus be studied on a cell-by-cell basis, permitting to perform statistical analyses of cellular populations and subpopulations. ColocalizR has been designed to parallelize tasks, making it applicable to the analysis of large data sets. Its graphical user interface makes it suitable for researchers without specific knowledge in image analysis. Moreover, results can be exported into a wide range of formats rendering post-analysis adaptable to statistical requirements. This application and its source code are freely available at https://github.com/kroemerlab/ColocalizR.

1. Introduction

Fluorescence microscopy has been evolving over the past decades, notably due to the emergence of novel ways to label cellular structures using molecular biology techniques (such as the fusion of proteins with green fluorescent protein (GFP) [1]) or chemical dyes (such as 4′,6-diamidino-2-phenylindole (DAPI), a fluorescent molecule that intercalates into DNA and therefore specifically stains nuclei). These techniques, which initially were used as tools for the morphological evaluation of cells [2], were rapidly employed for quantitative analysis thanks to the coevolution of image processing routines that allow for the extraction of numerous features related to intensity, morphology and texture (such as area, orientation, shape, average or standard deviation of intensity) [3], thus opening an avenue towards high-throughput analysis.

Today most image-analysis software (such as ImageJ [4,5], MetaMorph and CellProfiler [6]) or toolboxes (like the EBImage package in R [7] or the scikit-image from SciPy library [8,9] in Python) can "automatically" extract features on a cell-by-cell basis. However, one important exception from this general approach is the quantification of colocalization, *i.e.* the presence of two fluorescent signals in the same subcellular compartment. Most software packages still assess colocalization image by image in a way that is not compatible with the analysis of cell-based high-throughput assays. Standard colocalization methods have been criticized for their lack of reliability, mainly because single cells in the same population can exhibit opposing phenotypes [10] and even single-cell analysis can become challenging. For example, the Pearson correlation coefficient (PCC), which gives a measure of the pixel-by-pixel covariance, *i.e.* the co-distribution of two fluorescence signals within an image, can give rise to misinterpretation when large unlabeled extracellular regions (to be distinguished from background pixels) are included in the data for calculation.

* Corresponding author. Université Paris Descartes, Sorbonne Paris Cité, Paris, France.
E-mail address: kroemer@orange.fr (G. Kroemer).
[1] Contributed equally.

https://doi.org/10.1016/j.compbiomed.2019.02.024
Received 24 August 2018; Received in revised form 20 February 2019; Accepted 26 February 2019
0010-4825/

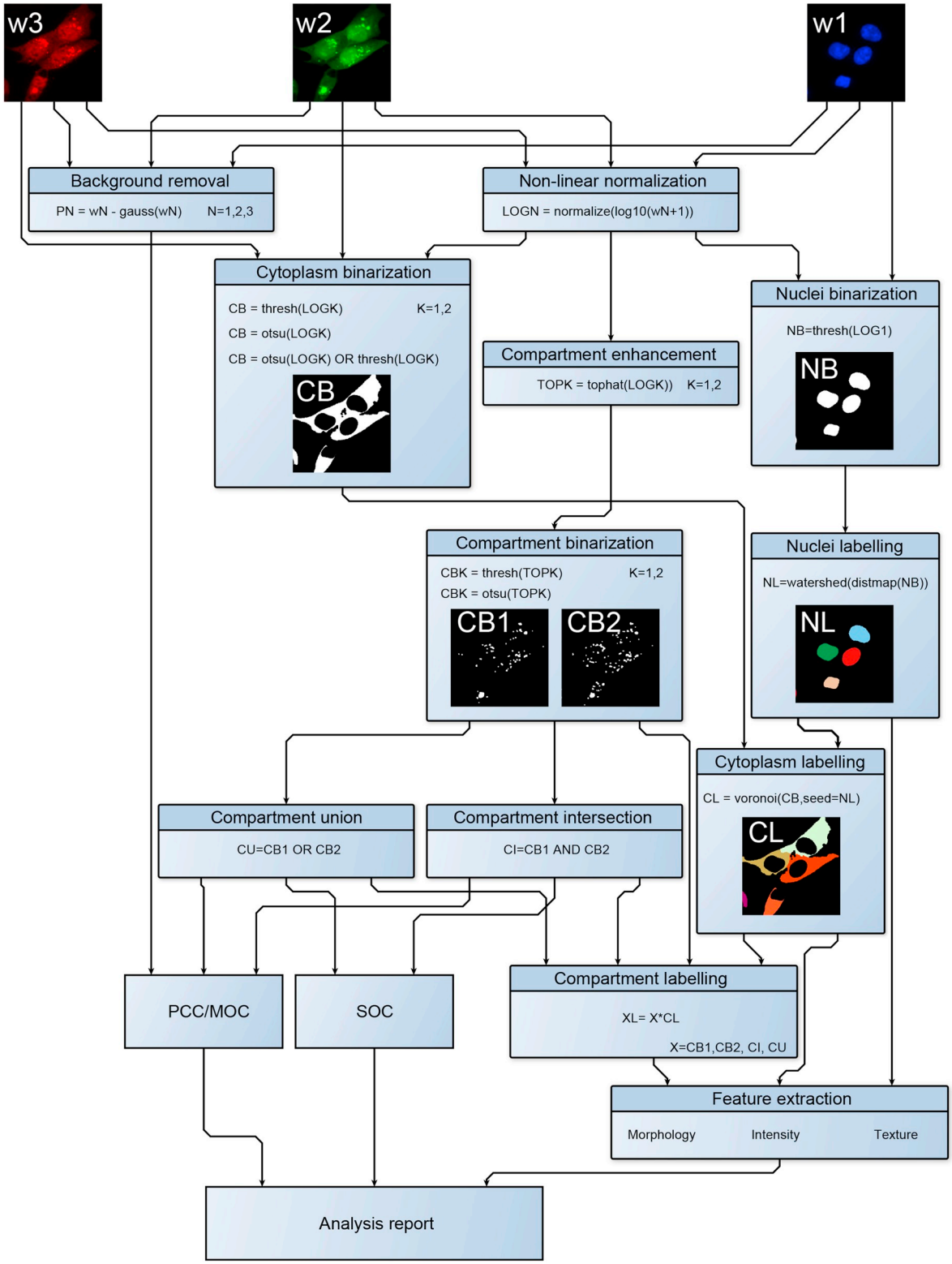

Fig. 1. ColocalizR image processing workflow. The main processing steps executed by ColocalizR are reported in a hierarchical diagram. Image processing operations are written in pseudo-code. gauss: Gaussian filter, thresh: adaptive threshold, tophat: top hat filter, otsu: Otsu binarization, voronoi: objects edges detection using Voronoi's method, AND/OR: Boolean operations, PCC: Pearson correlation coefficient, MOC: Manders overlap coefficient, SOC: surface overlap coefficient.

A cell-based colocalization analysis requires the combination of object-based and pixel-based colocalization methods, knowing that such methods are mostly used in a separate fashion [11]. We thus decided to develop the open-source application ColocalizR that enables population analysis by combining optimized cell-by-cell colocalization calculations at the organellar level, with the analysis of standard features related to intensity (including mean, standard deviation and quantile pixel intensity), morphology (such as area, perimeter and radius) as well as texture [12]. This R-based application mainly uses the EBImage package for image processing, and has been endowed with a

user-friendly Graphical User Interface (GUI) based on the shiny package [13]. ColocalizR is suitable for high-throughput analyses, has been optimized for CPU multithreading usage, and operates on multiple platforms; it can be easily installed and operated by any user, even without any specialized skills in image-analysis or programming.

ColocalizR was initially developed to assess the ability of certain lipophilic molecules, such as oleic acid, to induce the redistribution of red fluorescent protein (RFP) fused to MAP1LC3B (LC3) to the green fluorescent protein (GFP)-GALT1 marked Golgi apparatus and subsequent morphological changes [14,15]. We successfully applied ColocalizR to data obtained from a pharmacological drug screen and identified agents that induce a phenotype similar to the one caused by oleate. In addition, we used ColocalizR to analyze sets of images from different origin (such as the nucleoplasmic translocation of fibrillarin after inhibition of transcription), thus demonstrating its utility for analyzing diverse cellular phenotypes.

2. Material and methods

2.1. Cell culture & reagents

Human osteosarcoma U2OS biosensors cells that were either wild type or stably expressing the fluorescent fusion GALT1-GFP and RFP-LC3, were maintained at 37 °C, 5% CO_2, in Dulbecco's modified Eagle's medium (Thermo Fisher Scientific, Carlsbad, CA, USA) to which 10% fetal bovine serum (Gibco® by Life Technologies) was added. The Prestwick Chemical Library (PCL®) was purchased from Prestwick (Illkirch, France). Oleate was furnished by Larodan (Monroe, MI, USA). Cells were treated with 500 µM oleate dissolved in 100% ethanol, plus 10 and 30 µM of each of the 1280 compounds from the PCL®, for 6 h. Triplicates were performed for each condition. For transcription inhibition assays, cells were treated with 0.1 or 1 µM actinomycin D and BMH-21 for 2 h.

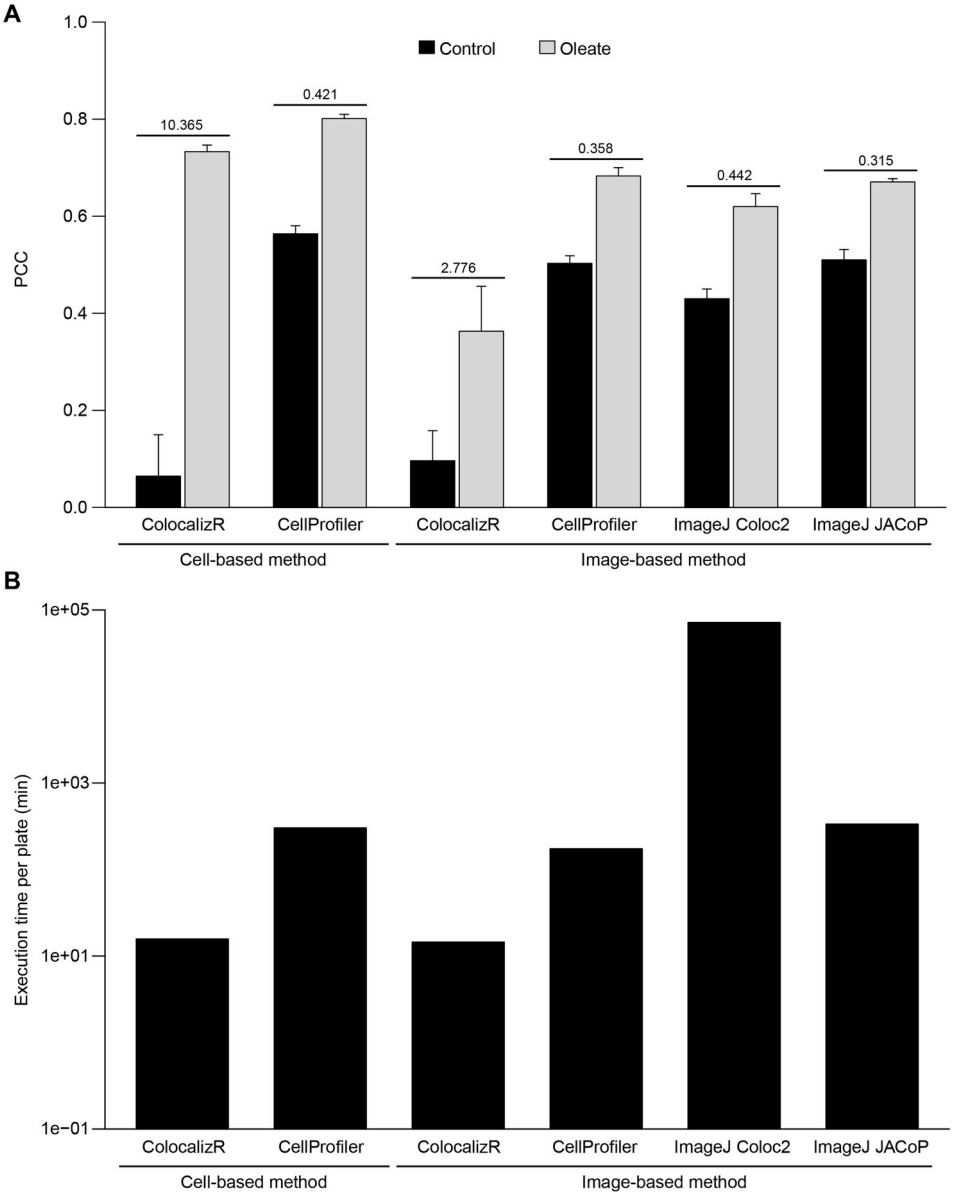

Fig. 2. Comparison of ColocalizR to traditional analytical methods. (**A, B**) Micrographs from oleate-treated or untreated cells were analyzed using either ColocalizR or other software methods, using both image-based and cell-based approaches when available. (**A**) Quantified PCC is reported in a bar chart. Relative increments are depicted for each condition. (**B**) Required time (hours in log) for analyzing one entire 384-well plate using each method is reported in a bar chart. Reported times for mono-threaded methods (Coloc2 and JACoP) were extrapolated from single-image analysis.

2.2. Image acquisition

U2OS cells were seeded in 384-well black microplates (Greiner-bio-one, Kremsmünster, Austria) and allowed to attach for 24 h (37 °C, 5% CO_2 atmosphere). Cells were fixed and stained after treatment in a 4% paraformaldehyde (PFA) solution containing 10 μg/mL Hoechst 33342 for 20 min, and thereafter rinsed twice with phosphate buffered saline (PBS). Images (four viewfields per well) were acquired on an ImageXpress Micro XL automated widefield microscope (Molecular Devices, Sunnyvale, CA, USA) using a CFI PlanApo Lambda 20X objective (Nikon, Tokyo, Japan) with a numerical aperture of 0.75.

Additional images of transcription inhibition were acquired on a TCS SPE microscope (Leica, Wetzlar, Germany) equipped with an ACS APO 63X oil objective with a numerical aperture of 1.3. Cells were fixed in PFA 3.5% and stained to visualize fibrillarin (FBL) and nucleoline (NCL) and counterstained with 4′,6-diamidino-2-phenylindole (DAPI) [16].

2.3. Image storage and compression

Images acquired on an ImageXpress MicroXL automated bioimager were stored as uncompressed MetaMorph 7.5 TIFF files with a pixel depth of 16 bits and a resolution of 5 MegaPixels (2160x2160 pixel matrix). Pixel size was 350 nm along both x and y axes. Images were also compressed using the lossless Lempel-Ziv-Welch (LZW) algorithm and tested without any impact on the results. Images were annotated following the nomenclature described in the ColocalizR user manual (available at https://github.com/kroemerlab/ColocalizR). Images acquired on a TCS SPE microscope in the LIF file format were converted into 16-bits TIFF files using the Bio-Format java library (https://www.openmicroscopy.org/bio-formats/). Of note, for the annotation of images not acquired by means of the Molecular Devices MetaMorph® software, applications such as *Bulk Rename Utility* (www.bulkrenameutility.co.uk) can be used.

2.4. Image segmentation

The ColocalizR analysis algorithm was developed to work with up to three fluorescence channels, to assess colocalization separately in the nuclear and the non-nuclear area (defined as cytoplasm) of each cell within an image. Single-cell objects were segmented based on nuclear staining. In the absence of nuclear staining the region-of-interest was defined as the entire cellular population. Of note, the cell-by-cell analysis permits a more accurate evaluation of colocalization, as it allows data cleaning (using features such as the Hoechst 33342 intensity for detecting and excluding dying or dividing cells from the analysis). In the first case, six masks were created from the original images: (i) nucleus, (ii) cytoplasm, (iii) signal from channel 1 (compartment 1), (iv) signal from channel 2 (compartment 2), (v) the union of iii and iv, (vi) the intersection of iii and iv (Fig. 1), using a previously described algorithm [17]. The main functionalities of the algorithm are described below.

(i) First, images were denoised by subtraction of background (obtained by applying a Gaussian filter on the original image [18,19]): the denoised images were used for PCC and MOC calculation only. Then signal heterogeneity was corrected by applying a non-linear normalization. Nuclear regions were detected and cleaned by applying an adaptive threshold (as described for the *thresh* function in the EBImage help documentation) [20–22], followed by successive opening and closing using a disc structuring element [23,24]. Nuclei were then separated and labelled by applying a watershed on the distance map [19,25] calculated from the previously obtained binary image (see the EBImage help documentation for more information). Alternatively a faster algorithm, based on the Voronoi method [26] which determines the nuclear borders based on a seed created from their erosion, can be used. An additional step of morphological filtering on the binary image, including a geodesic reconstruction [23,24] by dilation, followed by a geodesic reconstruction by erosion, both using a disc structuring element, can be added to eliminate small artifacts stemming from the segmentation.

(ii) The cytoplasm was detected using either first, second, or both grayscale signal channels. In the latter case, a combined image was calculated by averaging the two input images. By default, cytosolic regions were detected by binarization using the Otsu method [27]. This could be refined by means of an adaptive thresholding method, as described for the nuclear segmentation. Once defined, cytoplasmic regions were separated using the Voronoi method with the previously defined nuclear labelled mask as seed.

(iii) Finally, compartments, which can be defined as high-contrast subregions, were detected. A top hat filter [23] was applied to the original grayscale images, (which consists in subtracting their opening with a disc structuring element), to enhance high-contrast regions. After image histogram normalization [21], regions were binarized using either an Otsu, or an adaptive thresholding approach. Regions were labelled by multiplying the obtained binary image with the labelled cytoplasm mask.

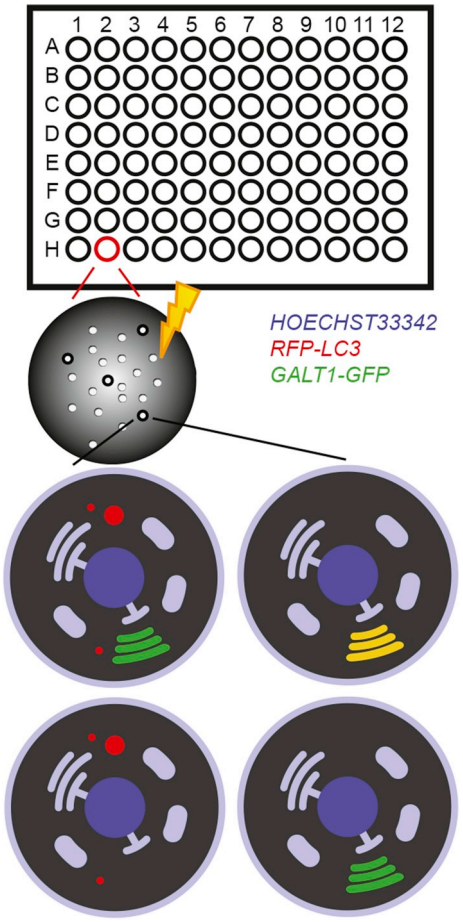

Fig. 3. Assessment of compartment dynamics. Upon exposure to drugs, cellular compartments can undergo morphological changes and their integrity can also be compromised. Upon treatment with some of the agents of the Prestwick library, the red fluorescent protein (RFP)-tagged LC3 protein redistributed to the green-fluorescent protein (GFF)-GALT1-labelled Golgi apparatus, leading ultimately (but not always) to the disruption of the Golgi apparatus with disappearance of the green fluorescence. (For interpretation of the references to colour in this figure legend, the reader is referred to the Web version of this article.)

Of note, the image-based approach followed the same steps, with the difference that it did not identify single cells.

2.5. Extraction of cellular features

After object labeling and linking [19], all features (intensity, morphology and texture) were calculated for masks i to iii (Fig. 1). These features are computed using the *ComputeFeatures* function from the EBImage package (see the help documentation for more information).

2.6. Calculation of colocalization parameters

ColocalizR was developed to provide a combination of intensity-based and object-based approaches by means of combining the assessment of colocalization by PCC, Manders overlap coefficient (MOC) or intensity correlation quotient (ICQ) [28–30], with an object detection algorithm. Colocalization was quantified in the cytoplasmic compartment using the masks v and vi as described in the previous section. For each cell, PCC, MOC and ICQ (which constitute a combination of pixel-based and object-based methods), were calculated by means of mask v, whereas the surface overlap coefficient (SOC), an object-based method quantifying the superimposition of two signals in the same pixel, was calculated using both masks v and vi. These parameters were defined as:

$$PCC = \frac{\sum (R_i - R_{Av}).\sum (G_i - G_{Av})}{\sqrt{\sum (R_i - R_{Av})^2.\sum (G_i - G_{Av})^2}} \quad (1)$$

$$ICQ = \frac{\sum (R_i > R_{Av}) = \sum (G_i > G_{Av})}{N_{pix}} - 0.5 \quad (2)$$

$$MOC = \frac{\sum (R_i).\sum (G_i)}{\sqrt{\sum (R_i)^2.\sum (G_i)^2}} \quad (3)$$

where R_i is the intensity of the first compartment (in red) in individual pixels and R_{Av} the arithmetic mean, whereas G_i and G_{Av} are the corresponding intensities for the second compartment (in green) in the same pixels.

$$SOC = \frac{\sum P_{G,i} \cap P_{R,i}}{\sum P_{G,i} \cup P_{R,i}} \quad (4)$$

where $P_{G,i}$ and $P_{R,i}$ correspond to the Boolean values indicating the absence (0) or the presence (1) of signal in a single pixel, in green and red channels respectively. Thus, $P_{G,i} \cap P_{R,i}$ equals 0 when there is no co-occurrence at a given pixel position (and 1 in the opposite case), and $P_{G,i} \cup P_{R,i}$ equals 0 in the absence of any signal at the same pixel position and 1 if at least one compartment is detected.

The fractional SOC for the green and red fluorescence (respectively named SOCG and SOCR) is also calculated, by replacing $P_{G,i} \cup P_{R,i}$ with $P_{G,i}$ or $P_{R,i}$ (thus replacing mask v with mask ii or iii).

2.7. Multithreading

In order to render colocalization analysis compatible with high throughput, we optimized the ColocalizR algorithm to take advantage of multithreaded hardware using the parallel, doParallel, foreach and snow R-packages [31–33]. This allowed minimizing the duration of calculation, allowing the assessment of a 384-well microtiter plate in 15 min by ColocalizR, versus 5 h using the JacoP plugin from imageJ (Fig. 2B).

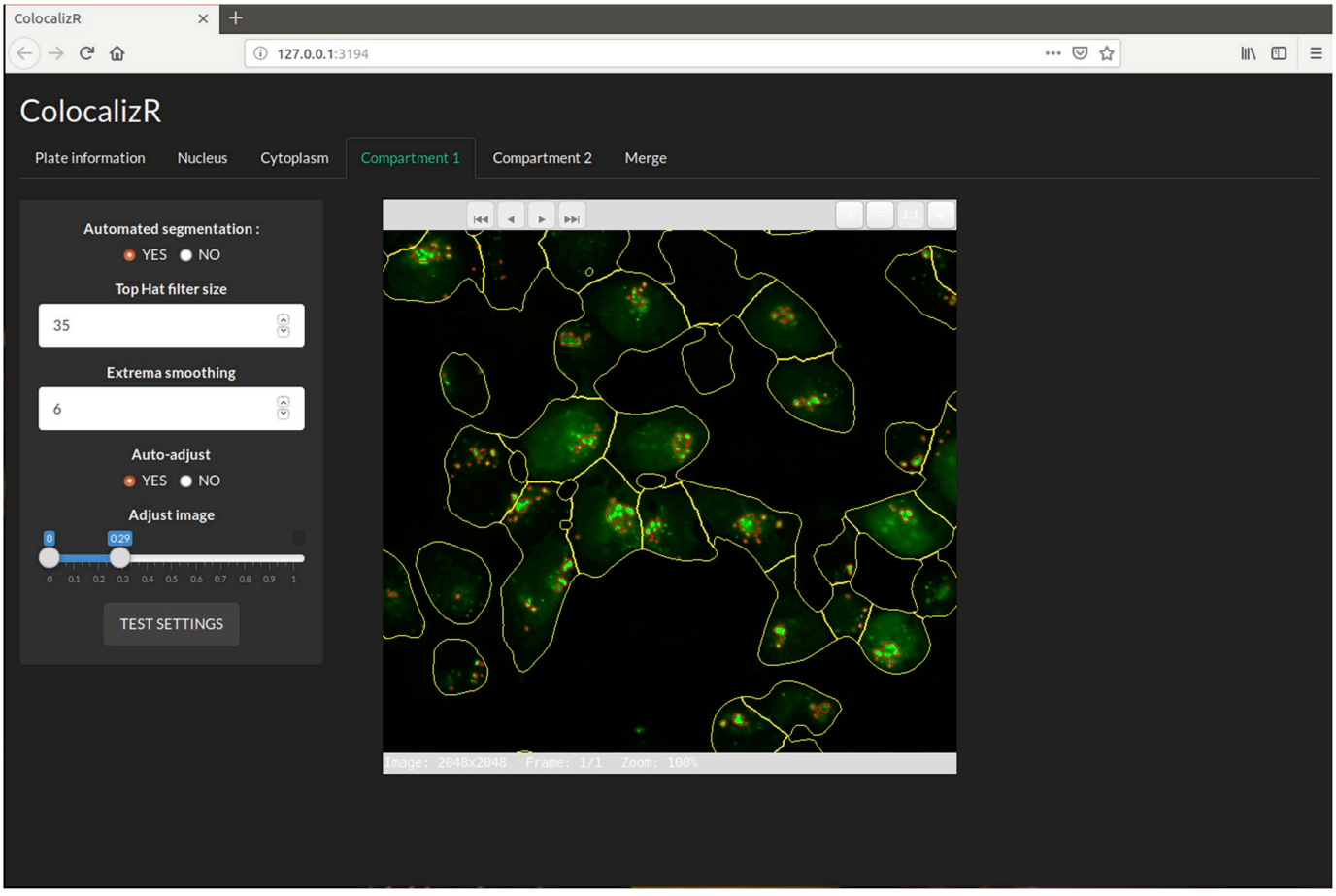

Fig. 4. Graphical user interface of ColocalizR.

2.8. Data processing and analysis

ColocalizR allows to export results in different file formats, namely, comma-separated values (csv), flow cytometry standard (fcs) or R data (rda). The first two options (csv and fcs) allowed for transferring data to other analytic software platforms. FlowJo® was used as a proof-of-concept tool for plotting bi-parametric graphs from exported fcs files. Routinely, we chose the third option (rda) to process data using R. Both ColocalizR analysis and further data processing were performed on a high-end computer equipped with an Intel Xeon E5-2620 v2 (16 threads) and 48 GB DDR3 RAM, running under Ubuntu 16.04.

3. Results

3.1. Combining pixel-based and object-based approaches improves assessment of colocalization

To develop an approach combining pixel-based and object-based colocalization methods for high-throughput analysis, we first focused on PCC, the gold-standard for colocalization assessment. We obtained microphotographs from untreated cells (negative control) that express two fluorescent biosensors, RFP-LC3 (marking autophagosomes and autolysosomes) and GALT1-GFP (marking the Golgi apparatus) in distinct cellular compartments, or from cells treated with oleate (positive control) causing partial coalescence of the two fluorescent signals. We then computed the PCC with ColocalizR's cell-based and image-based methods. Subsequently, we compared the results with the traditional method that measures pixel co-distribution across the whole image, with or without ROI detection (as image segments or cellular regions). For all methods but the cell-based one, we evaluated the average PCC in 4 viewfields; in the latter case, we calculated the mean of the modes from each of the 4 PCC distributions. ColocalizR yielded a better separation of positive and negative controls, especially when using the cell-based method, as compared to traditional analysis methods (Fig. S1). Using the same positive and negative controls, we then compared the speed and quality (characterized using relative increase calculation) of ColocalizR 's optimized cell-based and image-based methods with traditional software packages (CellProfiler, Coloc2 [34] & JACoP [30] ImageJ plugins). Once again, ColocalizR was superior in distinguishing positive and negative controls, as well as in calculating velocity as a result of multithread-orientated programming (Fig. 2).

3.2. Optimization of segmentation parameters

When added to cells that stably express RFP-LC3 and GALT1-GFP, oleate induced two distinct phenomena, namely (i) relocation of the autophagy-related fluorescence to the Golgi apparatus (resulting in the co-localization of RFP-LC3 and GALT1-GFP) and (ii) the disruption of the Golgi (leading to the reduction of the GALT1-GFP signal). Hence, upon oleate treatment four phenotypes were distinguished, based on the absence or presence of these two alterations (Fig. 3). It was therefore important to exclude cells with low GALT1-GFP signals (subsequent to the disruption of the Golgi) to avoid false positive PCC values. For this reason, a semi-automated adaptive thresholding method was applied to detect the GALT1-GFP signal, whereas RFP-LC3, which redistributed within the cell without major changes in its overall

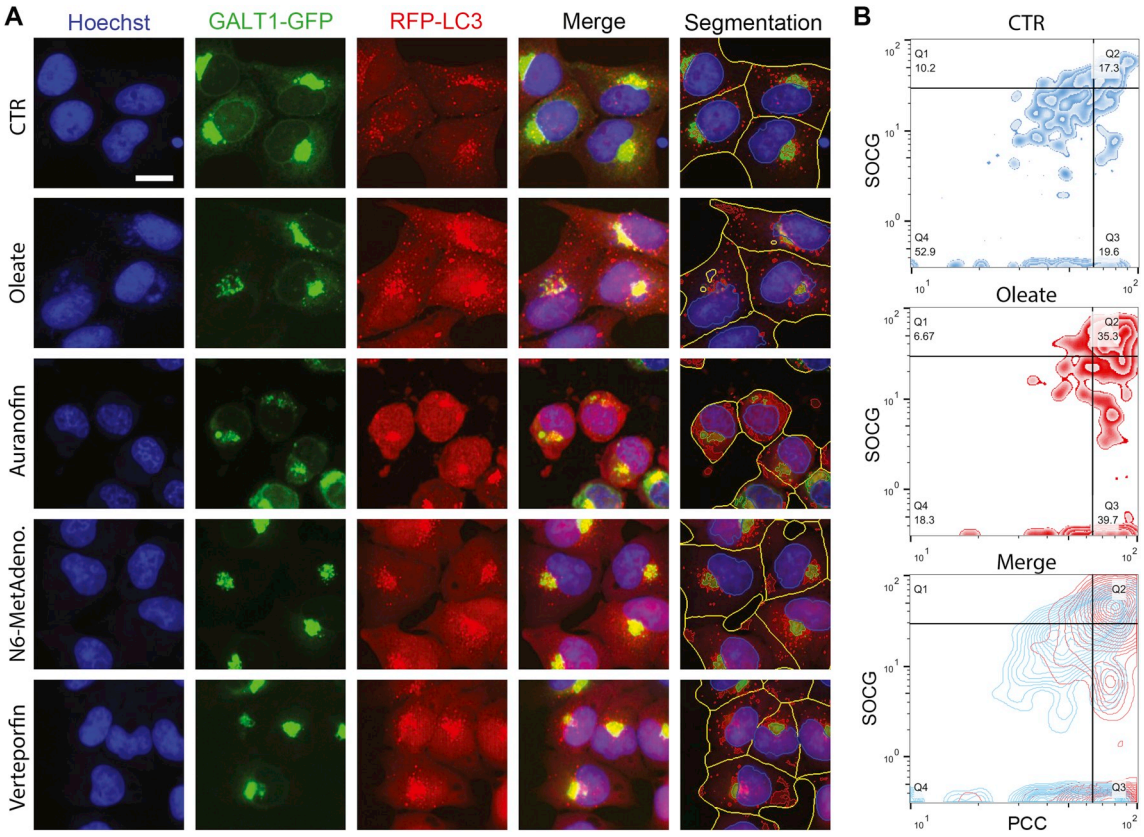

Fig. 5. Multiparametric colocalization analysis. (**A, B**) Cells stably expressing RFP-LC3 and GFP-GALT1 were treated with 500 μM oleate or compounds from the Prestwick library (10–30 μM) for 6 h. After fixation and nuclear counterstaining with Hoechst 33342, micrographs were taken and analyzed using ColocalizR. **A**. Representative images are depicted together with segmentation overlay for oleate-like compounds. Scale bar represents 10 μm **B**. The biparametric representation of cellular parameters is shown as density plot, displaying differences between the untreated control (blue) and the oleate treatment (red). (For interpretation of the references to colour in this figure legend, the reader is referred to the Web version of this article.)

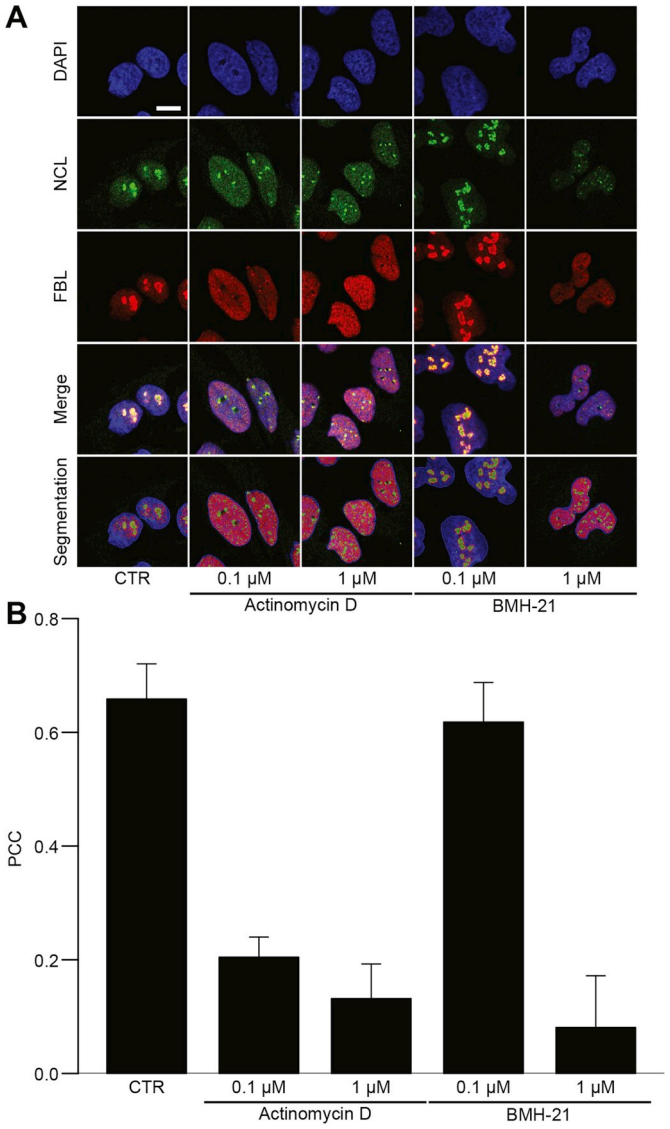

Fig. 6. Application of ColocalizR to a different biological system. (**A, B**) Cells were left untreated or treated with 0.1 and 1 μM actinomycin D or BMH-21 for 2 h, and then fixed. Nuclei were thereafter stained with DAPI, while FBL and NCL proteins were marked by immunofluorescence. The obtained images were analyzed using ColocalizR. (**A**) Representative images are depicted for each condition. The scale bar represents 10 μm. (**B**) The mean PCC ± SD are reported in a bar chart.

abundance, was detected using the automated Otsu method (Fig. 4). Of note, the calculation of morphological features by ColocalizR can be inactivated by the operator, thus accelerating the analysis process.

3.3. ColocalizR distinguishes between cellular phenotypes

No overt induction of cell death was detected following 6 h of treatment with oleate or other fatty acids. Nevertheless, dead (pyknotic) cells were removed from the analysis using nuclear morphological and intensity features [35]. PCC is the most robust parameter to detect cells that exhibit the colocalization of two fluorescent signals. However, PCC can result in a high false-positive rate due to structural changes in response to the treatment or the differential expression of the fluorescent protein. This obstacle was overcome by excluding cells that had a low GFP-GALT1 signal (SOCG close to 0) from the analysis (Fig. 5). Positive cells were therefore clustered as "positive" when they showed both high PCC and SOCG.

This method was applied for calculating the percentage of cells exhibiting GFP-LC3/RFP-GALT1 colocalization after exposing cells to 1280 distinct drugs from the Prestwick library. Manual thresholding and hierarchical clustering were used to identify compounds that induced phenotypic alterations similar to the ones induced by oleate. Using this approach, we identified 19 "oleate neighbors" that indeed caused the redistribution of LC3 to the Golgi apparatus (Fig. S2). Further studies performed on these "oleate neighbors" revealed that they all blocked protein secretion [36], underscoring their effects on endocrine and inflammatory circuitries [37]. Altogether, these results demonstrate that ColocalizR is applicable to drug screening campaigns.

3.4. ColocalizR is suitable for various image inputs

Next, we evaluated the capacity of ColocalizR to analyze images of various cellular markers acquired on a different microscope, in different file formats. NCL and FBL bind to the same nuclear granules in untreated control cells. When transcription of DNA into RNA is inhibited, NCL quickly leaks into other nuclear regions, hence separating from FBL, as determined by immunofluorescence. This subnuclear redistribution of the fluorescence was detectable by PCC analysis, revealing dose-dependent effects of actinomycin D and BMH-21, two well-known inhibitors of transcription (Fig. 6). These results suggest that ColocalizR can be used to analyze high-throughput chemical screen designed to identify novel transcription inhibitors.

4. Conclusion

Dynamic changes in the colocalization of fluorescent signals can occur as a response of individual cells (and cellular populations) to pharmacological agents. Here we developed ColocalizR, an application that facilitates the accurate and rapid analysis of colocalization data in a user-friendly, high-throughput fashion. Implemented in R, it can be easily installed, edited and executed, even if it cannot be used as a standalone application. Its originality resides in its simplicity that has been achieved by combining the EBImage package, which allows to build image analysis pipelines, with the shiny package, for creating a GUI. ColocalizR can consequently be used as a basis to build any kind of image analysis application. When implemented on a shiny server (Rstudio), it can also be implemented as an online tool. Of note, ColocalizR is able to automatically retrieve and analyze images acquired using a Molecular Devices IXM microscope on a local network, using the MetaxpR package (https://github.com/kroemerlab/MetaxpR), which can communicate with the MDCStore SQL database. It is able to quantify colocalization at the organellar level in large cellular populations, therefore increasing the statistical power as compared to other methods. ColocalizR can analyze a multitude of 5-MegaPixels-images within a limited time, meaning that this software is suitable for high-content analysis of high-throughput screens as they are used in pharmaceutical research.

Author contributions

Conceptualization, G.K., A.S. and M.L.; Methodology, G.K., A.S. and M.L.; Investigation, K.M. and A.S.; Formal Analysis, A.S and M.L.; Software, A.S. and M.L.; Writing – Original Draft, A.S. and M.L.; Writing –Review & Editing, O.K., G.K.; Funding Acquisition, G.K.; Supervision, O.K., G.K.

Acknowledgments

GK is supported by the Ligue Contre le Cancer (équipe labellisée); Agence National de la Recherche (ANR) – Projets blancs; ANR under the frame of E-Rare-2, the ERA-Net for Research on Rare Diseases; Association pour la Recherche sur le Cancer (ARC); Cancéropôle Île-de-France; Chancelerie des universités de Paris (Legs Poix), Fondation pour

la Recherche Médicale (FRM); a donation by Elior; the European Commission (ArtForce); European Research Area Network on Cardiovascular Diseases (ERA-CVD, MINOTAUR); the European Research Council (ERC); Fondation Carrefour; Institut National Du Cancer (INCa); Inserm (HTE); Institut Universitaire de France; LeDucq Foundation; the LabEx Immuno-Oncology; the RHU Torino Lumière; the Seerave Foundation; the SIRIC Stratified Oncology Cell DNA Repair and Tumor Immune Elimination (SOCRATE); and the SIRIC Cancer Research and Personalized Medicine (CARPEM). We are grateful to Frederique Maczkowiak for providing microphotographs from the transcription inhibition assay.

Appendix A. Supplementary data

Supplementary data to this article can be found online at https://doi.org/10.1016/j.compbiomed.2019.02.024.

References

[1] M. Chalfie, et al., Green fluorescent protein as a marker for gene expression, Science 263 (5148) (1994) 802–805.
[2] M. Renz, Fluorescence microscopy - a historical and technical perspective, Cytometry 83 (9) (2013) 767–779.
[3] E. Glory, R.F. Murphy, Automated subcellular location determination and high-throughput microscopy, Dev. Cell 12 (1) (2007) 7–16.
[4] C.A. Schneider, W.S. Rasband, K.W. Eliceiri, NIH Image to ImageJ: 25 years of image analysis, Nat. Methods 9 (7) (2012) 671.
[5] C.T. Rueden, et al., ImageJ2: ImageJ for the next generation of scientific image data, BMC Bioinf. 18 (1) (2017) 529.
[6] A.E. Carpenter, et al., CellProfiler: image analysis software for identifying and quantifying cell phenotypes, Genome Biol. 7 (10) (2006) R100.
[7] G. Pau, et al., EBImage - an R package for image processing with applications to cellular phenotypes, Bioinformatics 26 (7) (2010) 979–981.
[8] E. Jones, et al., SciPy: Open Source Scientific Tools for Python, (2001).
[9] S. Van der Walt, et al., Scikit-image: image processing in Python, PeerJ 2 (2014) e453.
[10] K.W. Dunn, M.M. Kamocka, J.H. McDonald, A practical guide to evaluating colocalization in biological microscopy, Am. J. Physiol. Cell Physiol. 300 (4) (2011) C723–C742.
[11] B. Moser, et al., Fluorescence colocalization microscopy analysis can be improved by combining object-recognition with pixel-intensity-correlation, Biotechnol. J. 12 (1) (2017) 1600332.
[12] R.M. Haralick, K. Shanmugam, I. Dinstein, Textural features for image classification, IEEE Trans. Syst. Man Cybern. 3 (6) (1973) 610–621 SMC.
[13] W. Chang, et al., Shiny: Web Application Framework for R, (2018).
[14] L.C. Gomes-da-Silva, et al., Photodynamic therapy with redaporfin targets the endoplasmic reticulum and Golgi apparatus, EMBO J. (2018) e98354.
[15] M. Niso-Santano, et al., Unsaturated fatty acids induce non-canonical autophagy, EMBO J. 34 (8) (2015) 1025–1041.
[16] L. Colis, et al., DNA intercalator BMH-21 inhibits RNA polymerase I independent of DNA damage response, Oncotarget 5 (12) (2014) 4361–4369.
[17] A. Sauvat, et al., Automated analysis of fluorescence colocalization: application to mitophagy, Methods in Enzymology, Elsevier, 2017, pp. 219–230.
[18] J.C. Russ, Designing kernels for image filtering, J. Comput. Assist. Microsc. 7 (4) (1995) 179–190.
[19] J.C. Russ, The Image Processing Handbook, CRC press, 2016.
[20] J.C. Russ, Thresholding images, J. Comput. Assist. Microsc. 7 (3) (1995) 141–164.
[21] A.K. Jain, Fundamentals of Digital Image Processing, Prentice Hall, Englewood Cliffs, NJ, 1989.
[22] R.C. Gonzales, P. Wintz, Digital Image Processing, Addison-Wesley, 1987.
[23] L. Najman, H. Talbot, Introduction to Mathematical Morphology. Mathematical Morphology: from Theory to Applications, (2013), pp. 1–33.
[24] J. Serra, P. Soille, Mathematical Morphology and its Applications to Image Processing vol. 2, Springer Science & Business Media, 2012.
[25] G. Bertrand, et al., Watersheds in Discrete Spaces. Mathematical Morphology: from Theory to Applications, (2013), pp. 81–107.
[26] T.R. Jones, A. Carpenter, P. Golland, Voronoi-based segmentation of cells on image manifolds, Computer Vision for Biomedical Image Applications, Springer Berlin Heidelberg, Berlin, Heidelberg, 2005.
[27] N. Otsu, A threshold selection method from gray-level histograms, IEEE Trans. Syst. Man Cybern. 9 (1) (1979) 62–66.
[28] J. Adler, I. Parmryd, Quantifying colocalization by correlation: the Pearson correlation coefficient is superior to the Mander's overlap coefficient, Cytometry 77 (8) (2010) 733–742.
[29] F.P. Cordelieres, S. Bolte, Experimenters' guide to colocalization studies: finding a way through indicators and quantifiers, in practice, Methods in Cell Biology, Elsevier, 2014, pp. 395–408.
[30] S. Bolte, F. Cordelieres, A guided tour into subcellular colocalization analysis in light microscopy, J. Microsc. 224 (3) (2006) 213–232.
[31] M. Corporation, S. Weston, doParallel: Foreach Parallel Adaptor for the 'parallel' Package, (2017).
[32] Microsoft, S. Weston, Foreach: Provides Foreach Looping Construct for R, (2017).
[33] L. Tierney, et al., Snow: Simple Network of Workstations, (2016).
[34] J. Schindelin, et al., Fiji: an open-source platform for biological-image analysis, Nat. Methods 9 (7) (2012) 676.
[35] L. Burgoyne, The mechanisms of pyknosis: hypercondensation and death, Exp. Cell Res. 248 (1) (1999) 214–222.
[36] L. Zhao, et al., Identification of pharmacological inhibitors of conventional protein secretion, Sci. Rep. 8 (1) (2018) 14966.
[37] R.A. Baumgartner, V.A. Deramo, M.A. Beaven, Constitutive and inducible mechanisms for synthesis and release of cytokines in immune cell lines, J. Immunol. 157 (9) (1996) 4087–4093.